Autophagy 6:6, 764-776; August 16, 2010; © 2010 Landes Bioscience

Characterization of autophagosome formation site by a hierarchical analysis of mammalian Atg proteins

Eisuke Itakura and Noboru Mizushima*

Department of Physiology and Cell Biology; Tokyo Medical and Dental University; Bunkyo-ku, Tokyo Japan

Key words: autophagosome, PI3-kinase, isolation membrane, endoplasmic reticulum, ULK

Abbreviations: PI3-kinase, phosphatidylinositol 3-kinase; PAS, pre-autophagosomal structure; CVT, cytoplasm-to-vacuole targeting; DFCP1, double FYVE domain-containing protein 1; FIP200, focal adhesion kinase family interacting protein of 200 kD; KO, knockout; LC3, microtubule-associated protein 1 light chain 3; MEF, mouse embryonic fibroblast; mRFP, monomeric red fluorescent protein; ULK1, unc-51-like kinase 1; VMP1, vacuole membrane protein 1; WIPI, WD-repeat protein interacting with phosphoinosides

Autophagy is an intracellular degradation process, through which cytosolic materials are delivered to the lysosome. Despite recent identification of many autophagy-related genes, how autophagosomes are generated remains unclear. Here, we examined the hierarchical relationships among mammalian Atg proteins. Under starvation conditions, ULK1, Atg14, WIPI-1, LC3 and Atg16L1 target to the same compartment, whereas DFCP1 localizes adjacently to these Atg proteins. In terms of puncta formation, the protein complex including ULK1 and FIP200 is the most upstream unit and is required for puncta formation of the Atg14-containing PI3-kinase complex. Puncta formation of both DFCP1 and WIPI-1 requires FIP200 and Atg14. The Atg12-Atg5-Atg16L1 complex and LC3 are downstream units among these factors. The punctate structures containing upstream Atg proteins such as ULK1 and Atg14 tightly associate with the ER, where the ER protein vacuole membrane protein 1 (VMP1) also transiently localizes. These structures are formed even when cells are treated with wortmannin to suppress autophagosome formation. These hierarchical analyses suggest that ULK1, Atg14 and VMP1 localize to the ER-associated autophagosome formation sites in a PI3-kinase activity-independent manner.

Introduction

Macroautophagy (which we will simply refer to as autophagy) is a unique form of membrane-mediated trafficking, which delivers macromolecules and organelles from the cytoplasm to lysosomes for degradation. At the first step of autophagy, cytoplasmic constituents including organelles are sequestered by a unique membrane cisterna called the isolation membrane/phagophore. Complete sequestration results in the formation of an autophagosome. The autophagosome fuses with a lysosome to become an autolysosome, in which lysosomal hydrolases digest the internal contents to metabolites that are released back into the cytosol for recycling.

Autophagy is an evolutionarily conserved process from yeast to mammals. It is important for a number of physiological processes such as adaptation to starvation, preimplantation embryo development, prevention of neurodegeneration, anti-aging mechanisms, tumor suppression, degradation of invading microorganisms and presentation of intracellular antigens.[1-6]

Autophagosome formation is mainly governed by autophagy-related (Atg) proteins. To date, more than 30 *ATG* genes have been identified in yeast, which are involved not only in starvation-induced autophagy, but also in the cytoplasm-to-vacuole targeting (Cvt) pathway, a constitutive biosynthetic pathway that delivers two vacuolar enzymes, aminopeptidase 1 (Ape1) and α-mannnosidase (Ams1), to the autophagosome, and special types of autophagy such as pexophagy and mitophagy. Among these, 15 genes (*ATG1-10, 12-14, 16* and *18*) are required for all types of autophagy.[7-9] In addition to this set, starvation-induced macroautophagy also requires *ATG17, 29* and *31*. The Atg proteins play essential roles in autophagosome formation and are classified into six functional complexes/groups: (i) the Atg1 kinase complex (Atg1-13-17-29-31); (ii) Atg9; (iii) the class III phosphatidylinositol (PI) 3-kinase complex (Atg6/Vps30-Atg14-Vps15-Vps34); (iv) the PI(3)P-binding Atg2-Atg18 complex; (v) the Atg12 conjugation system (Atg12-Atg5); and (vi) the Atg8 conjugation system involving phosphatidylethanolamine (Atg8-PE).[8,10] The hierarchical relationship between these Atg proteins has also been determined (**Suppl. Fig. 1**).

Identification of the origin of the autophagosome has been a long-standing question.[9] It has been proposed that the

*Correspondence to: Noboru Mizushima; Email: nmizu.phy2@tmd.ac.jp
Submitted: 03/30/10; Revised: 06/03/10; Accepted: 06/18/10
Previously published online: www.landesbioscience.com/journals/autophagy/article/12709

autophagosome is derived from a ribosome-free region of the rough ER or some post-Golgi membrane,[11,12] or is assembled de novo.[13] In yeast, the putative autophagosome formation site has been identified; almost all Atg proteins gather at a perivacuolar compartment, called the pre-autophagosomal structure (PAS).[14,15] A live cell imaging experiment showed that autophagosomes are indeed generated from this structure.[14] However, the precise nature of the PAS remains unknown.

In mammals, almost all Atg proteins are conserved.[9,16,17] Mammalian target of rapamycin (mTOR) complex 1 (mTORC1) interacts with and regulates a multimeric complex made up of unc-51-like kinase 1 (ULK1, an Atg1 homologue), Atg13, focal adhesion kinase family interacting protein of 200 kD (FIP200, a putative functional counterpart of Atg17) and Atg101.[18-24] The autophagy-specific class III PI3-kinase complex was also recently identified as a Beclin 1 (Atg6/Vps30 homologue)-Atg14-Vps34-Vps15 complex.[25-28] Atg18 homologues are known as WIPI (WD-repeat protein interacting with phosphoinosides) family proteins (WIPI-1-4).[29] The two conjugation systems—the Atg12 system and the Atg8/LC3 (microtubule-associated protein light chain 3) system—are also well conserved in mammals.[30] However, hierarchal relationships between these mammalian Atg proteins have not yet been fully established. For example, interdependency of the ULK1 complex and the autophagy-specific class III PI3-kinase complex (Beclin 1-Atg14-Vps34-Vps15) is not clear.

Additionally, a PAS-equivalent structure has not yet been described in mammalian cells, which limits our understanding of autophagosome formation in mammalian cells. Recently, Ktistakis's group discovered that a novel PI(3)P-binding protein termed double FYVE-containing protein 1 (DFCP1), whose homologue is absent in yeast, translocates to a subdomain of the ER and generates the "omegasome" during starvation.[31] LC3-positive structures are generated at or in close proximity to this DFCP1-positive omegasome. This important discovery suggests that a certain subdomain of the ER plays a critical role in autophagosome formation in mammalian cells. More recently, direct connection between isolation membrane and the ER has been demonstrated.[32,33] However, characterization of this subdomain and the relationship between DFCP1 and other Atg proteins remains to be determined.

In this study, in order to characterize the autophagosome formation site in mammalian cells, we first determined hierarchical relationships among the mammalian Atg proteins including DFCP1 using a combination of various Atg-deficient cell lines and the PI3-kinase inhibitor wortmannin. The most upstream factor was the ULK1-FIP200 complex, followed by the Atg14-containing PI3-kinase complex. Puncta formation of the other downstream factors including DFCP1 was dependent on the ULK1 complex and PI3-kinase activity. Based on these findings, we further analyzed the localization of the upstream factors and found that ULK1 and Atg14 punctate structures tightly associate with the ER membrane. Vacuole membrane protein 1 (VMP1) also localizes to the site of autophagosome formation independently of the other Atg proteins. These sites may represent autophagosome formation sites in mammalian cells.

Results

ULK1, Atg14, WIPI-1, Atg16L1 and LC3 co-localize to the same punctate structures in close proximity to the DFCP1 puncta during starvation. Analyses of mammalian Atg proteins have identified at least three critical protein complexes: the ULK1-Atg13-FIP200-Atg101 complex, the Beclin 1-Atg14-Vps34-Vps15 (class III PI3-kinase) complex and the Atg12-Atg5-Atg16L1 complex. Additionally, WIPI-1, LC3 and DFCP1 are also involved in autophagosome generation. We first examined the localization of representative factors from each group (ULK1, Atg14, Atg16L1, WIPI-1, LC3 and DFCP1) under starvation conditions using antibodies against endogenous proteins or cells stably expressing GFP- or HA-tagged proteins.

While these Atg proteins showed only small numbers of punctate structures under normal growing conditions (**Suppl. Fig. 2A**), their numbers increased during starvation. As we previously observed,[18,25] ULK1 and Atg14 puncta almost completely co-localized with Atg16L1 (98.1% ± 1.2% of the ULK1 puncta are positive for Atg16L1) (**Fig. 1A and Suppl. Fig. 2B**). Since Atg16L1 and Atg5 can serve as markers for the isolation membrane (**Suppl. Fig. 2C**),[34] these ULK1 and Atg14 puncta primarily represent isolation membranes. Indeed, the ULK1 dots co-localized well with Atg14 (92.6% ± 2.8% of the ULK1 puncta are positive for Atg14) (**Fig. 1B**).

WIPI-1, an Atg18 homologue, was previously shown to co-localize with LC3.[29] Our analysis revealed that, while only a part of the LC3 puncta co-localized with WIPI-1 as well as Atg14 (43.7% ± 1.8% of the LC3 puncta are positive for WIPI-1) (**Suppl. Fig. 2D and E**), WIPI-1 co-localized well with Atg14 and Atg16L1 (81.6% ± 3.6% of the Atg14 puncta are positive for WIPI-1, 98.5% ± 0.6% of the Atg16L1 puncta are positive for WIPI-1 and 69.8% ± 2.8% of the WIPI-1 puncta are positive for Atg16L1) (**Fig. 1C and D**), suggesting that WIPI-1 primarily exists on the isolation membrane, rather than the complete autophagosome (LC3-positive).

We next examined the localization of DFCP1. DFCP1 is an ER-associating FYVE domain-containing protein, and translocates upon starvation to subdomains of the ER called omegasomes, which are in close proximity to the LC3 and Vps34 puncta.[31] Only 47.8% ± 2.1% of the LC3 structures were positive for DFCP1, while 83.3% ± 3.5% DFCP1 structures were positive for LC3, again suggesting that DFCP1 is absent on mature autophagosomes (**Fig. 1F**). Consistent with this previous report, we found that most of the GFP-DFCP1 puncta were present in very close proximity to, rather than completely co-localized with, the Atg16L1, Atg14 and WIPI-1 (another PI(3)P-binding protein) puncta (**Fig. 1E, G–I and L**).

Co-localization of these proteins shown in **Figure 1** is graphically displayed in linescan plots (**Fig. 1J and K, and Suppl. Fig. 3**). These results suggest that upon autophagy induction, ULK1, Atg14, WIPI-1, LC3 and Atg16L1 target to the same compartment, which is most likely an isolation membrane, and DFCP1 localizes adjacent to these Atg proteins.

The LC3 and Atg12 systems functions downstream of FIP200 and PI3-kinase. We next determined hierarchical

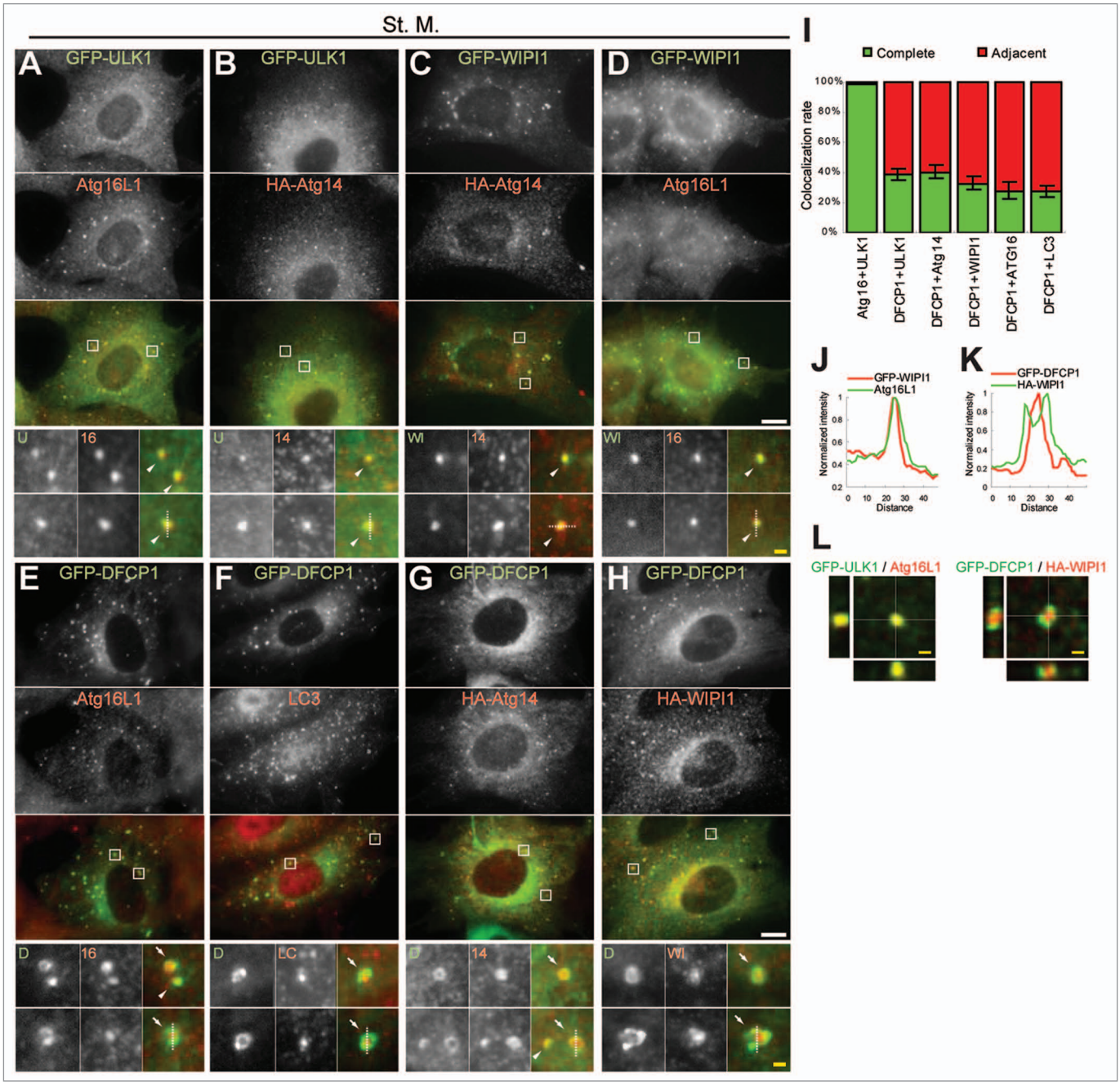

Figure 1. ULK1, Atg14, WIPI-1, Atg16L1 and LC3 co-localize to the same compartment, which is in close proximity to the DFCP1 structure. (A–H) Mouse embryonic fibroblasts (MEFs) stably expressing GFP-ULK1 (A), GFP-ULK1 and HA-Atg14 (B), HA-Atg14 and GFP-WIPI-1 (C), HA-WIPI-1 (D), GFP-DFCP1 (E and F), GFP-DFCP1 and HA-Atg14 (G) and GFP-DFCP1 and HA-WIPI-1 (H) were cultured in starvation medium for 1 hour. Cells were then fixed, permeabilized, and subjected to immunofluorescence microscopy using anti-HA (B, C, G and H), anti-Atg16L1 (A, D and E) and anti-LC3 antibodies (F). Due to low expression, GFP-ULK1 and GFP-DFCP1 were stained with anti-GFP antibodies. Nearly complete co-localization is indicated by arrowheads and adjacent co-localization is indicated by arrows. The structures indicated with broken lines were subjected to linescan analysis (shown in J, K and Suppl. Fig. 3). Signal color is indicated by color of typeface. St. M., starvation medium. Scale bars, 10 μm (white) and 1 μm (yellow). (I) Quantification of complete and adjacent co-localization between indicated Atg protein pairs after 1-hour starvation. Data represent mean ± SE of ten images. (J–K) Linescans were obtained from representative punctate structures showing co-localization between GFP-WIPI-1 and Atg16L1 (J) and between HA-WIPI-1 and GFP-DFCP1 (K). Original structures are shown in (D and H) (indicated with dashed lines). (L) 3D reconstruction of Atg puntate structures. 1-hour starved cells were observed by confocal laser microscopy and then 3D images were reconstituted. Lateral images reconstituted from Z-sectioning are also shown. Scale bars, 1 μm.

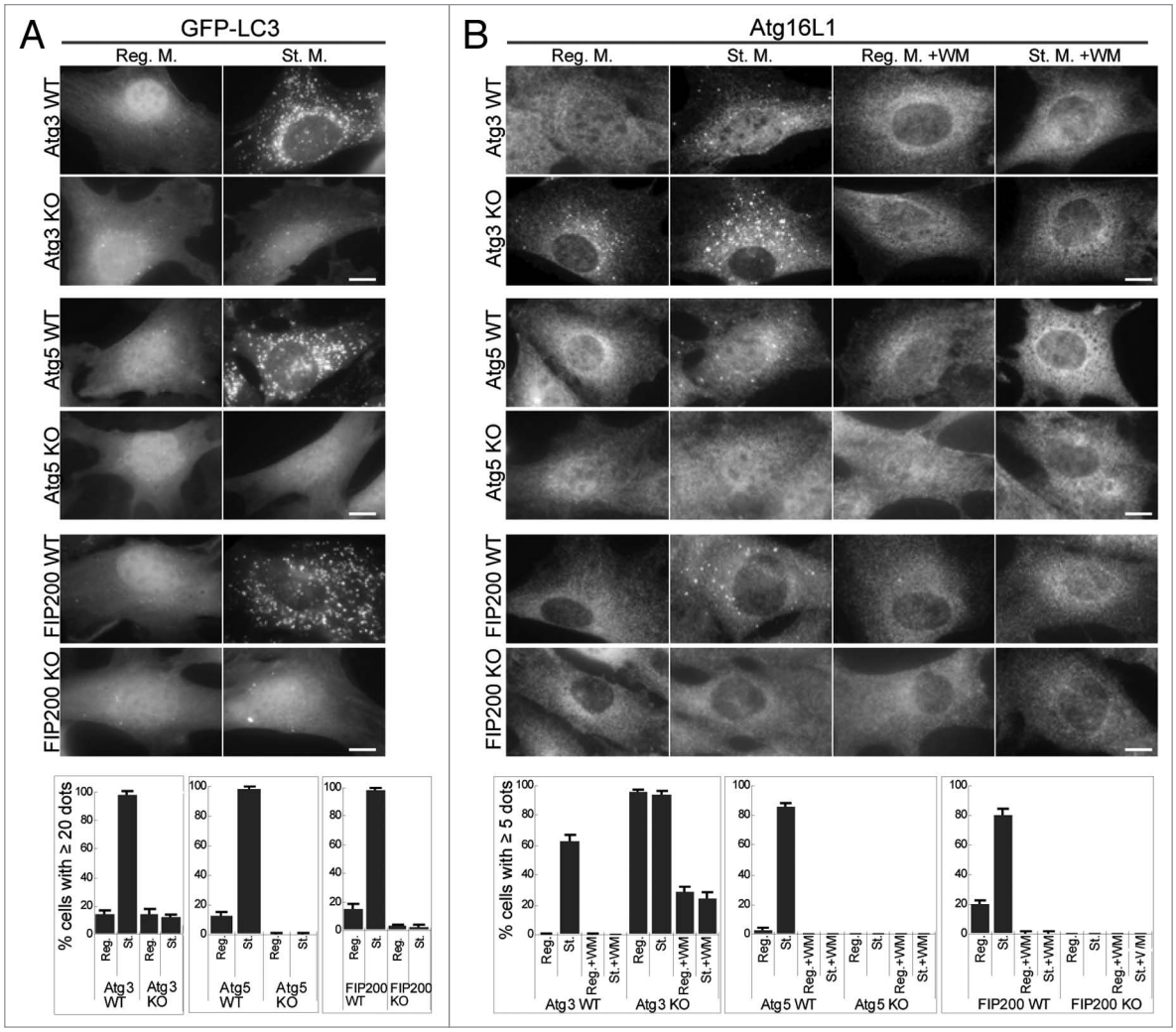

Figure 2. Localization of GFP-LC3 and endogenous Atg16L1 in Atg3 KO, Atg5 KO and FIP200 KO MEFs. Puncta formation of GFP-LC3 (A) and endogenous Atg16L1 (B) was assessed in Atg3 KO, Atg5 KO and FIP200 KO MEFs, and wortmannin-treated cells. Wild-type MEFs and MEFs deficient for Atg3, Atg5 and FIP200 stably expressing GFP-LC3 were cultured in regular or starvation medium, with or without 0.2 μM wortmannin for 2 hours. Cells were then fixed and examined by fluorescence microscopy. For Atg16L1 detection, cells were stained with anti-Atg16L1 antibodies. Scale bars, 10 μm. Graphs show the results of quantification of the dot positive cells (more than 20 dots (A) and 5 dots (B) per cell). Results shown represent mean ± SE of triplicate samples containing greater than 100 cells. Reg. M., regular medium; St. M., starvation medium; WM, wortmannin; WT, wild-type.

relationships of mammalian Atg proteins as performed in yeast cells (**Suppl. Fig. 1**).[10] To this end, we used mouse embryonic fibroblast (MEF) clones deficient for Atg3 (an E2 enzyme required for LC3-PE conjugation), Atg5 and FIP200 to inhibit functions of the LC3 and Atg12 conjugation systems, and the ULK1 complex, respectively. We transfected wild-type, Atg3 KO, Atg5 KO and FIP200 KO MEF clones with HA-WIPI-1, GFP-DFCP1, GFP-Atg14, GFP-ULK1 and GFP-LC3, and generated transformants stably expressing each construct. We examined the localization of these tagged proteins in regular or starvation medium, with or without wortmannin, an inhibitor of PI3-kinase.

First, as a part of this comprehensive hierarchical analysis, we analyzed starvation-induced puncta formation of LC3 and Atg16L1, most of which have already been reported in previous studies. LC3 puncta formation was suppressed in Atg3 KO, Atg5 KO and FIP200 KO MEFs (**Fig. 2A**).[18,34,35] Formation of endogenous Atg16L1 puncta formation was also inhibited in Atg5 knockout (KO) cells,[34] FIP200 KO cells and wortmannin-treated cells (**Fig. 2B**), but was enhanced in Atg3 KO cells, even when cultured in the regular medium (**Fig. 2B**).[35] These results confirm that the Atg12-Atg5-Atg16L1 complex functions upstream of the LC3 system and downstream of the ULK1 and PI3-kinase complexes.

Formation of both WIPI-1 and DFCP1 structures is regulated by the ULK1-FIP200 and Atg14-PI3-kinase complexes. WIPI-1 is a PI(3)P-binding protein and its puncta formation was suppressed by wortmannin in wild-type cells, as previously reported (**Fig. 3A**).[29] Its puncta formation was also inhibited in FIP200 KO cells (**Fig. 3A**). However, in Atg3 KO and Atg5 KO cells, an increased number of WIPI-1 puncta were generated, even under nutrient-rich conditions, and numbers further increased following starvation (**Fig. 3A**). Accumulation of these WIPI-1

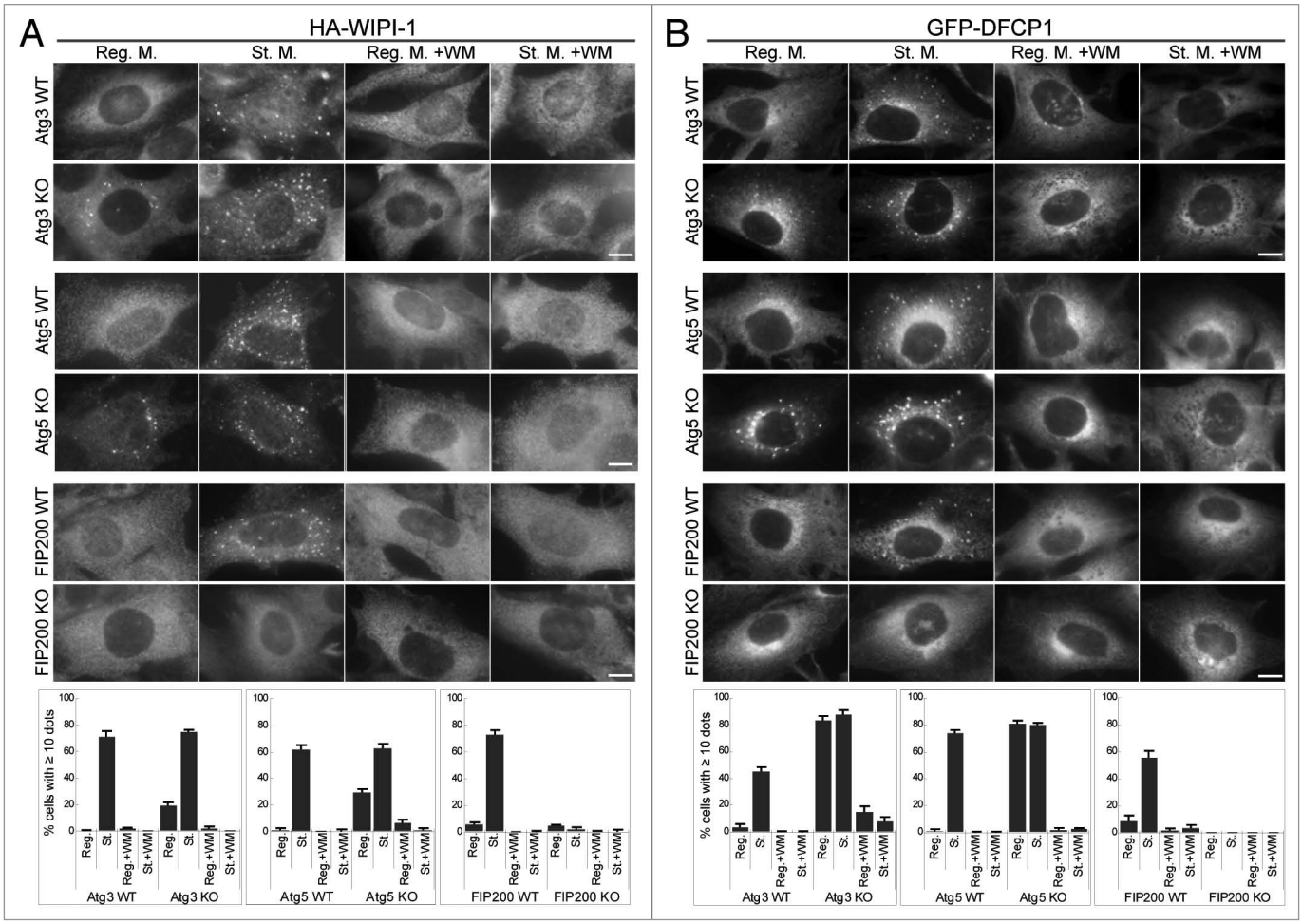

Figure 3. Puncta formation of the PI(3)P-binding proteins WIPI-1 and DFCP1 is defective in FIP200 KO MEFs and wortmannin-treated cells. MEFs deficient for Atg3, Atg5 and FIP200, and their corresponding wild-type control MEFs stably transformed with HA-WIPI-1 (A) or GFP-DFCP1 (B) were cultured in regular or starvation medium, with or without 0.2 μM wortmannin for 1 hour. Cells were then fixed, permeabilized, and subjected to immunofluorescence microscopy using anti-HA (A) or anti-GFP antibodies (B). Graphs show the results of quantification of dot positive cells. The Y axis indicates % cells demonstrating more than 10 dots. Results shown represent mean ± SE of triplicate samples containing greater than 100 cells. Reg. M., regular medium; St. M., starvation medium; WM, wortmannin; WT, wild-type. Scale bars, 10 μm.

puncta was inhibited by wortmannin (**Fig. 3A**). Thus, WIPI-1 should function downstream of the ULK1 and PI3-kinase complexes, and likely upstream of the Atg12-Atg5-Atg16L1 complex and LC3.

It has been reported that DFCP1 localizes to the omegasome during starvation, and this translocation is dependent on the FYVE domain of DFCP1.[31] Consistent with this report, DFCP1 showed primarily reticular and Golgi-like patterns under nutrient-rich conditions, and DFCP1 puncta became apparent following starvation, a process which was sensitive to wortmannin (**Fig. 3B**). In contrast, a comparable number of these DFCP1 puncta were already present, even under nutrient-rich conditions in Atg3 KO and Atg5 KO cells (**Fig. 3B**). Formation of these dots was inhibited by wortmannin, ruling out the possibility that these could be nonphysiological aggregation. Finally, the DFCP1 puncta formation was completely inhibited in FIP200 KO cells, even during starvation (**Fig. 3B**). These data suggest that, like WIPI-1, DFCP1 functions upstream of the Atg12-Atg5-Atg16L1 complex and LC3, and downstream of the ULK1 and PI3-kinase complexes.

There are at least two class III PI3-kinase complexes in mammalian cells. The Beclin 1-Atg14-Vps34-Vps15 complex is important for autophagy, whereas the Beclin 1-UVRAG (Vps38)-Vps34-Vps15 complex, which occasionally includes Rubicon, is important for regulation of endocytosis.[25-28] We therefore determined whether localization of WIPI-1 and DFCP1 is indeed dependent on the autophagy-specific PI3-kinase complex. Treatments of cells with siRNAs against Vps34 and Atg14 suppressed puncta formation of both WIPI-1 (**Fig. 4A**) and DFCP1 (**Fig. 4B**). These results suggest that both WIPI-1 and DFCP1 are bona fide effectors of the autophagy-related PI3-kinase, although they are not co-localized with each other (**Fig. 1H**).

Formation of Atg14 puncta depends on the ULK1-FIP200 complex. We previously found that Atg14 puncta formation was resistant to wortmannin treatment.[25] Atg14 puncta formation was also not affected in Atg3 KO and Atg5 KO cells, even in

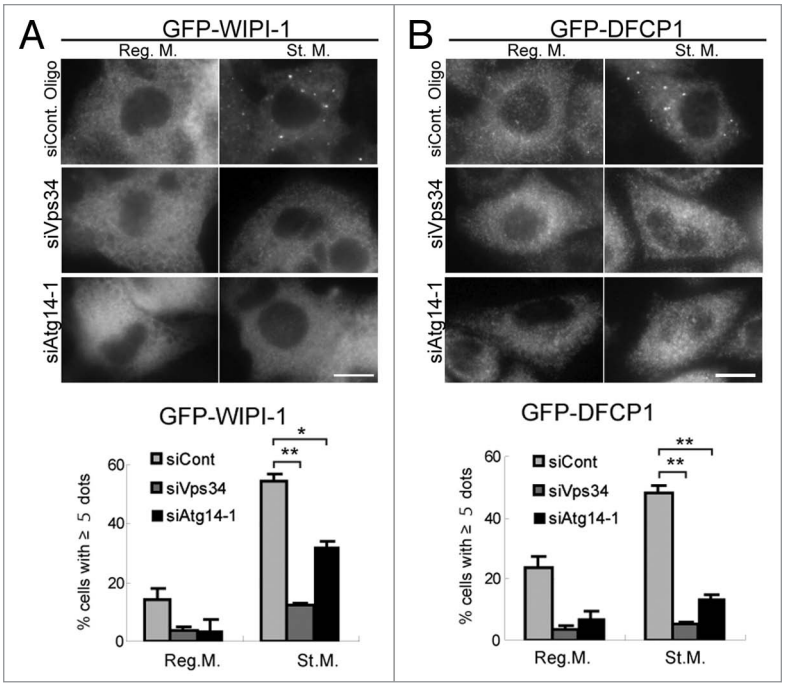

Figure 4. Puncta formation of WIPI-1 and DFCP1 depends on Atg14 and Vps34. HepG2 cells stably expressing GFP-WIPI-1 (A) and HeLa cells stably expressing GFP-DFCP1 (B) were treated with Atg14, Vps34 or control siRNA oligos, as indicated. Cells were cultured in starvation medium for 2 hours, and then subjected to immunofluorescence microscopy using anti-GFP antibodies. Graphs show the results of quantification of the GFP dot positive cells (more than 5 dots per cell). Results shown represent mean ± SE of triplicate samples containing greater than 100 cells. *p < 0.05, **p < 0.01, Student t-test. Reg. M., regular medium; St. M., starvation medium. Scale bars, 10 μm.

the presence of wortmannin (**Fig. 5A**). However, these punctate structures were not observed in FIP200 KO cells, suggesting that the Atg14-containing PI3-kinase complex functions downstream of the ULK1 complex, and upstream of the Atg12-Atg5-Atg16L1 complex and LC3.

Formation of the ULK1 punctate structures showed a pattern similar to that of the Atg14 puncta. The ULK1 puncta formation was wortmannin-resistant and not affected by deletion of Atg3 and Atg5 in the presence of wortmannin (**Fig. 5B**). However, as we previously reported, ULK1 puncta were not observed in Atg5 KO MEFs if wortmannin was not added.[18] It may be possible that ULK1 rapidly dissociates from autophagosome intermediate structures in Atg5 KO cells, but could remain on the intermediate structures when autophagosome formation is blocked at an earlier step by wortmannin treatment. Our present data suggest that Atg5 is not essential for generation of the ULK1 puncta, but could be important for keeping ULK1 on the membrane. As previously observed, FIP200 was required for ULK1 puncta formation as a binding partner.[18]

Taken together, these results of the hierarchical analyses of the mammalian Atg proteins are summarized in **Figure 5C**. The ULK1-FIP200 complex appears to be the most upstream factor, followed by the Atg14-containing PI3-kinase complex, their putative effectors (DFCP1 and WIPI-1), the Atg12-Atg5-Atg16L1 complex and LC3.

Early autophagic structures tightly associate with the ER membrane. While wortmannin suppresses formation of the isolation membrane[36] and omegasome,[31] it does not affect the localization of ULK1 and Atg14 (**Fig. 5**). In the presence of wortmannin, ULK1 still co-localized with Atg14, suggesting that these dots could represent functional intermediate structures (**Fig. 6A**). We previously reported that Atg14 puncta co-localized with Vps34 in starved cells,[25] and this co-localization was also maintained in wortmannin-treated cells (**Fig. 6B**). These data imply that the ULK1 and Atg14 punctate structures observed in the presence of wortmannin could represent early autophagic structures located at autophagosome formation sites.

There has been accumulating evidence that the ER is involved in autophagosome formation: The omegasome is derived from the ER,[31] and there are direct connections between isolation membrane and the ER.[32,33] We, therefore, examined the relationship between the ULK1 puncta and the ER. In cells stably transformed with HA-ULK1, ULK1 puncta were frequently associating with the ER (**Fig. 6C**). In live-cell imaging experiments, the GFP-ULK1 puncta were present on or in close proximity to the ER and moved together with the ER reticular structures (**Fig. 6D and Suppl. Video 1**). This association was also observed in wortmannin-treated cells (**Fig. 6E and Suppl. Video 2**). Neither GM130 (a cis-Golgi marker) nor Lamp1 (a late endosome/lysosome marker) co-localized with the ULK1-Atg14 puncta (**Suppl. Fig. 4A–C**). In addition, most ULK1 puncta did not co-localize with TOM70 (a mitochondria marker) (**Suppl. Fig. 4D**). These data suggest that ULK1 and Atg14 target to the early autophagic structures on or in close proximity to the ER before a step that requires PI3-kinase activity.

VMP1 localizes to the early autophagic structure, but functions at a later step of autophagosome formation. ULK1 puncta may localize to certain subdomains of the ER. We tested whether these sites represent known structures on or close to the ER, however, ULK1 did not co-localize with Sec23A (an ER-exit site marker) or ERGIC-53 (an ER-Golgi intermediate compartment, ERGIC, marker) (**Suppl. Fig. 4E and F**).

It is known that VMP1, an ER-associated transmembrane protein, is involved in autophagosome formation and interacts with Beclin 1.[37] VMP1 was originally identified as a pancreatitis-induced protein, which is absent in yeast.[38] Dictyostelium VMP1 is required for autophagosome formation as well as for integrity/biogenesis of various other organelles.[39,40] We speculated that VMP1 could also target to the autophagosome formation site. To determine the precise subcellular localization of VMP1, we generated MEFs stably expressing VMP1-GFP. VMP1 was observed at a perinuclear Golgi-like structure and reticular structures throughout the cytoplasm (**Fig. 7A**). We also confirmed that VMP1 was co-fractionated primarily with protein disulfide isomerase (an ER marker), and with syntaxin 6 (a Golgi marker) on an OptiPrep density gradient (**Fig. 7B**). On

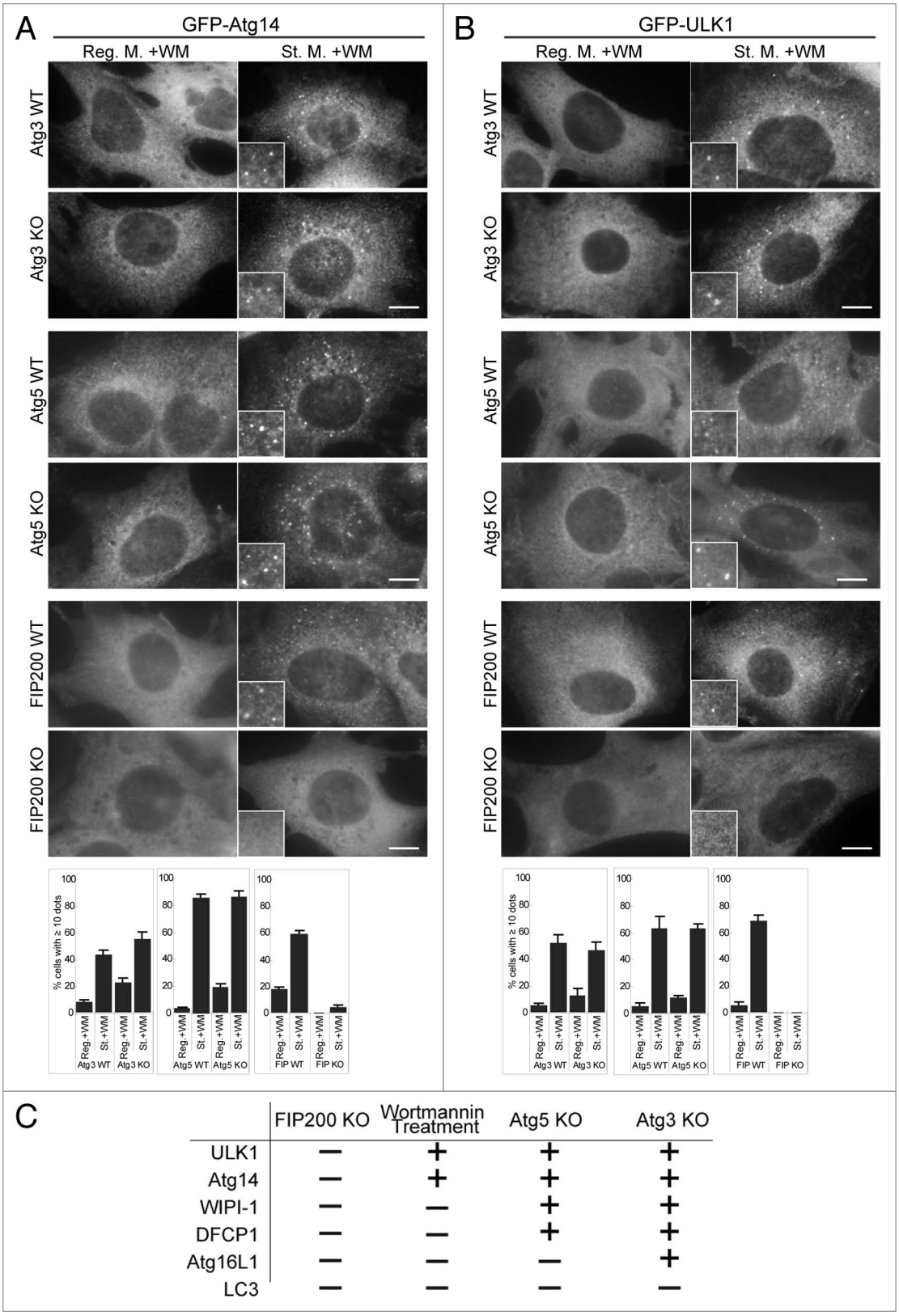

Figure 5. Wortmannin-resistant ULK1 and Atg14 puncta are generated in Atg3 KO and Atg5 KO cells, but not in FIP200 KO cells. (A and B) MEFs deficient for Atg3, Atg5 and FIP200, and their corresponding wild-type control MEFs, stably expressing GFP-Atg14 (A) or GFP-ULK1 (B) were cultured in regular or starvation medium with 0.2 μM wortmannin for 1 hour. Cells were then subjected to immunofluorescence microscopy using anti-GFP antibodies. Graphs show the results of quantification of the GFP dot positive cells (more than 10 dots per cell). Results shown represent mean ± SE of triplicate samples containing greater than 100 cells. Reg. M., regular medium; St. M., starvation medium; WM, wortmannin; WT, wild-type. Scale bars, 10 μm. (C) Summary of the hierarchy analysis of mammalian Atg proteins in terms of puncta formation. "+" and "-" indicate whether puncta were formed or not formed, respectively.

the other hand, the majority of Beclin 1 was not co-fractionated with VMP1.

In contrast to a previous report showing that VMP1 puncta appear following starvation,[37] we detected punctate VMP1 structures even under nutrient-rich conditions. This is not due to constitutive activation of autophagy by VMP1-GFP overexpression, because ULK1 puncta were induced only following starvation (**Fig. 7C and D**). These VMP1 puncta were associated

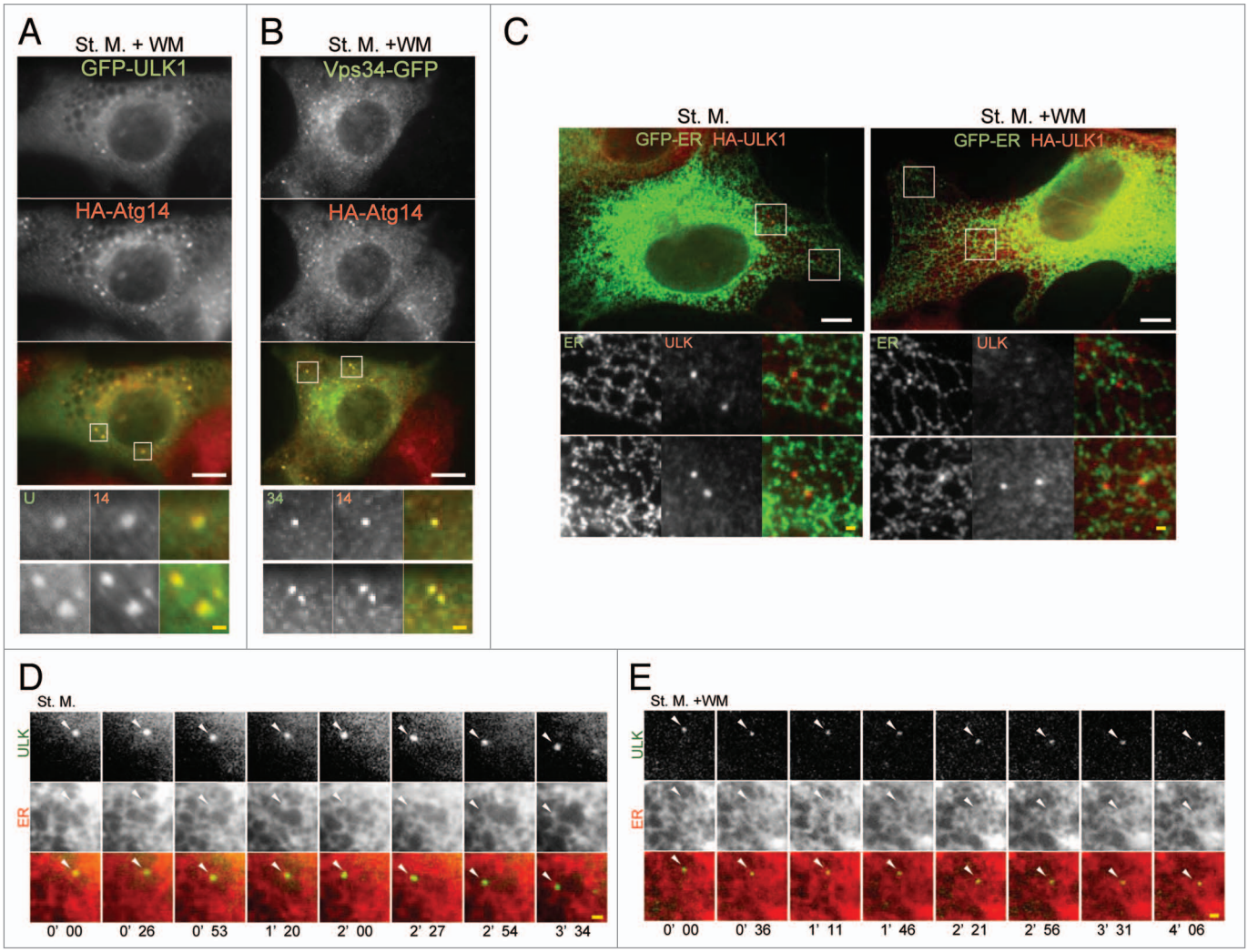

Figure 6. ULK1 puncta tightly associate with the ER membrane. (A and B) NIH3T3 cells stably expressing GFP-ULK1 (A) or Vps34-GFP (B) together with HA-Atg14 were cultured in starvation medium with 0.2 μM wortmannin for 1 hour. Cells were then fixed, permeabilized, and subjected to immunofluorescence microscopy using anti-HA and anti-GFP (for GFP-ULK1) antibodies. Signal color is indicated by color of typeface. St. M., starvation medium; WM, wortmannin. Scale bars, 10 μm (white) and 1 μm (yellow). (C) MEFs stably expressing GFP-ER (containing transmembrane region of rat cytochrome b5) and HA-ULK1 were cultured in starvation medium, with or without 0.2 μM wortmannin for 1 hour, and then subjected to immunofluorescence microscopy using anti-GFP and anti-HA antibodies. (D and E) Selected frames from time-lapse movies of MEFs stably expressing GFP-ULK1 and mRFP-ER in starvation medium, with (E) or without (D) 0.2 μM wortmannin are shown. The cells were imaged starting from 30 minutes (D) or 90 minutes (E) after the starvation treatment commenced. Localization of GFP-ULK1 is indicated by arrowheads. See Video 1 and 2 for whole images. Signal color is indicated by color of typeface. St. M., starvation medium; WM, wortmannin. Scale bars, 10 μm (white) and 1 μm (yellow).

with the ER network (**Fig. 7A**). Under starvation conditions, the VMP1 puncta were not increased in number, and showed very little co-localization with ULK1 (approximately 5% of the ULK1 puncta are positive for VMP1) (**Fig. 7D and F**). However, following the wortmannin treatment, approximately 50% of the ULK1 puncta co-localized with VMP1 (**Fig. 7E and F**). These results suggest that VMP1 transiently associates with the early autophagic structures, and dissociates from them in a PI3-kinase-dependent manner.

We next examined the hierarchical relationship between ULK1 and VMP1. The VMP1 puncta were generated and became larger in FIP200 KO cells compared to in wild-type cells (**Fig. 7G**), even though the ER structure remained intact in FIP200 KO cells (**Suppl. Fig. 5A**). This indicates that VMP1 could be an upstream factor of the ULK1 complex. However, VMP1 silencing did not block the puncta formation of ULK1; rather, it induced abnormally large structures positive for ULK1, WIPI-1, DFCP1 and Atg16L1 (**Fig. 7H, Suppl. Fig. 5B**). p62, a selective autophagic substrate,[41] accumulated and became resistant to starvation-induced degradation and lysosomes-dependent LC3 turnover was impaired in VMP1 siRNA-treated cells, confirming that autophagic degradation is indeed blocked in these cells (**Fig. 7I**). These data suggest that VMP1 is not required for recruitment of ULK1, WIPI-1, DFCP1 and Atg16L, but appears to play an important role in maturation/turnover of the autophagic structures at a later step.

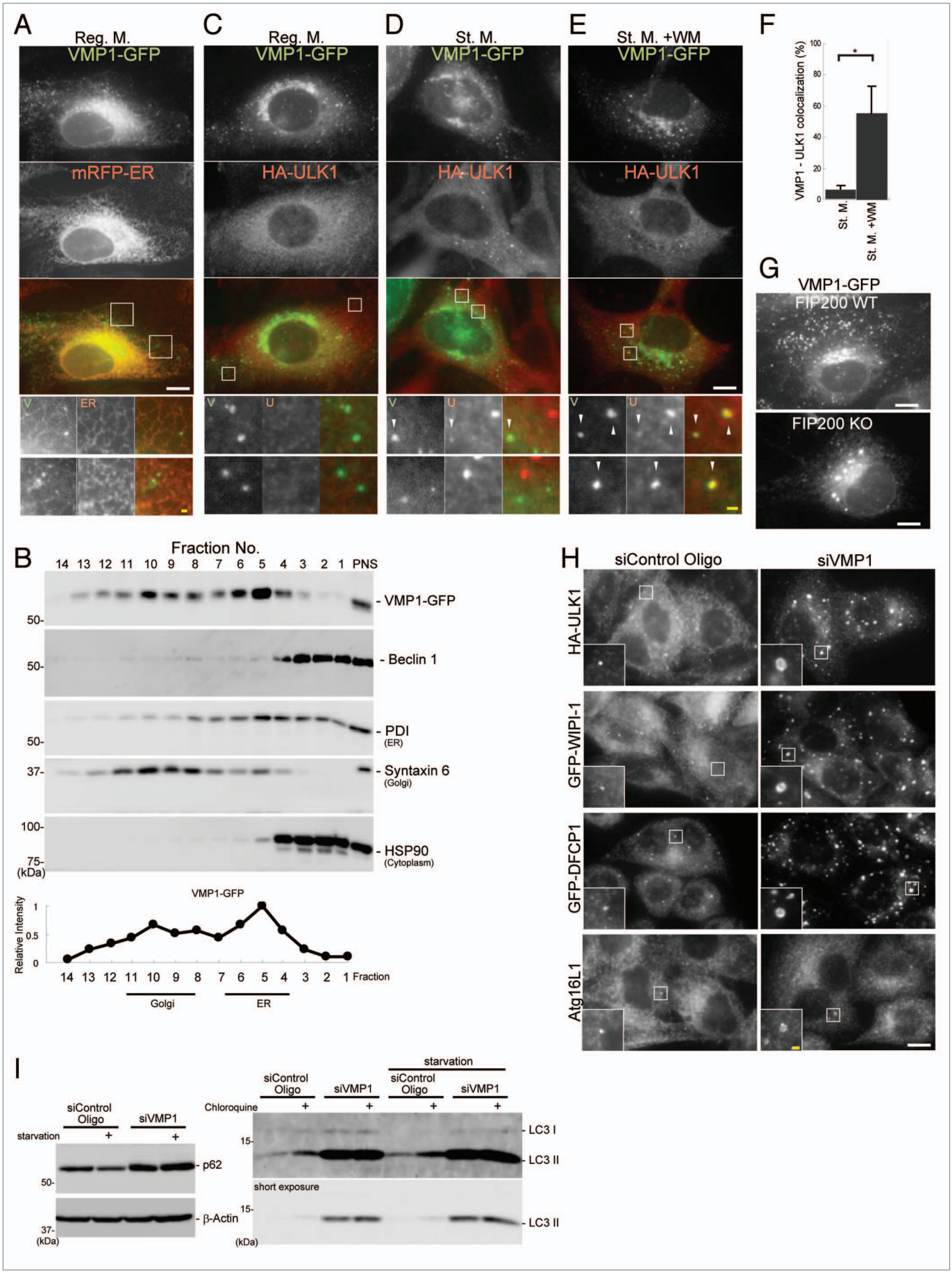
A
Reg. M.
VMP1-GFP
mRFP-ER
V
ER
C
Reg. M.
VMP1-GFP
HA-ULK1
V
U
D
St. M.
VMP1-GFP
HA-ULK1
V
U
E
St. M. +WM
VMP1-GFP
HA-ULK1
V
U
F
VMP1 - ULK1 colocalization (%)
100
80
60
40
20
0
*
St. M.
St. M. +WM
G
VMP1-GFP
FIP200 WT
FIP200 KO
B
Fraction No.
14 13 12 11 10 9 8 7 6 5 4 3 2 1 PNS
- VMP1-GFP
50-
- Beclin 1
50-
- PDI
(ER)
50-
- Syntaxin 6
(Golgi)
37-
- HSP90
(Cytoplasm)
100-
75-
(kDa)
VMP1-GFP
Relative Intensity
1
0.5
0
14 13 12 11 10 9 8 7 6 5 4 3 2 1 Fraction
Golgi
ER
H
siControl Oligo
siVMP1
HA-ULK1
GFP-WIPI-1
GFP-DFCP1
Atg16L1
I
siControl Oligo
siVMP1
starvation
+
+
p62
50-
β-Actin
37-
(kDa)
starvation
siControl Oligo
siVMP1
siControl Oligo
siVMP1
Chloroquine
+
+
+
+
15-
LC3 I
LC3 II
short exposure
15-
LC3 II
(kDa)

Figure 7 (See previous page). VMP1 localizes to the early autophagic structure. (A and C–E) MEFs stably expressing VMP1-GFP and RFP-ER or HA-ULK1 were cultured in regular or starvation medium, with or without 0.2 μM wortmannin for 1 hour. Cells were subjected to immunofluorescence microscopy using anti-HA antibodies. Colocalization between VMP1 and ULK1 is indicated by arrowheads. (B) MEFs stably expressing VMP1-GFP were cultured in regular medium and subjected to subcellular fractionation as described in Materials and Methods. Immunoblot analysis showed the distribution of VMP1-GFP, Beclin 1, protein disulfide isomerase (PDI, ER marker), syntaxin 6 (Golgi marker) and HSP90 (cytoplasmic protein marker). (F) Graph shows the result of quantification of colocalization between VMP1 and ULK1. The Y axis indicates VMP1-positivity (%) of the ULK1 puncta. Results shown represent mean ± SE of 10 cells. *$p < 0.01$, Student's t-test. (G) Wild-type and FIP200 KO MEFs stably expressing VMP1-GFP were observed under nutrient-rich conditions. (H) HeLa cells stably expressing HA-ULK1, GFP-WIPI-1 and GFP-DFCP1 were treated with VMP1 or control siRNA oligos. Cells were cultured in starvation medium for 1 hour, and then subjected to immunofluorescence microscopy using anti-HA, anti-GFP and anti-Atg16L1 antibodies. Signal color (A and C–E) is indicated by color of typeface. Reg. M., regular medium; St. M., starvation medium; WM, wortmannin. Scale bars, 10 μm (white) and 1 μm (yellow). (I) HeLa cells were treated with VMP1 or control siRNA oligos, as indicated. Cells were cultured in starvation medium for 2 hours with or without 20 mM choloroquine and then starvation-induced p62 degradation and lysosomes-dependent LC3 turnover was determined by immunblot analysis.

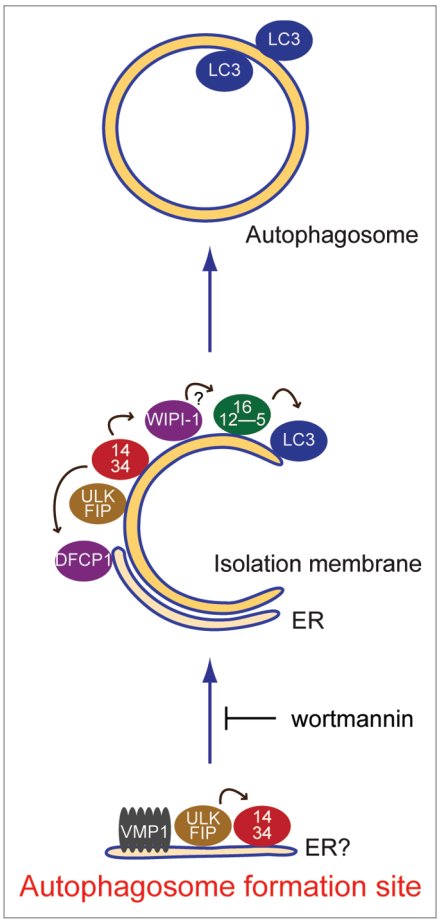

Figure 8. Model of autophagosome formation and hierarchical relationship among mammalian autophagy proteins. At the initial step, the ULK1 and Atg14 complexes localize to the autophagosome formation sites, which are on or in close proximity to the ER. VMP1 also transiently associates with this structure. Wortmannin treatment causes accumulation of the ULK1-Atg14-VMP1 structures, suggesting that dissociation, but not formation, of this structure depends on PI3-kinase activity. Downstream of this step, the two PI(3)P binding proteins WIPI-1 and DFCP1, the Atg12-Atg5-Atg16L1 complex and LC3-PE function to appropriately elongate the isolation membrane. The arrows indicate interdependency among the mammalian Atg proteins for puncta formation.

Discussion

We examined the intracellular localization of ULK1, Atg14, DFCP1, WIPI-1, Atg16L and LC3 in this study. Together with our previous studies on Atg13, FIP200, Atg101, Vps34, Atg12 and Atg5, these data suggest that almost all mammalian Atg proteins except DFCP1 accumulate at the same compartments upon induction of autophagy. Although DFCP1 puncta show a unique pattern, they are always in close proximity to these Atg structures. This is consistent with a previous report demonstrating that DFCP1-labeled omegasomes co-localize adjacently with LC3, Atg5 and Vps34 puncta.[31]

We then analyzed the hierarchical relationships among these mammalian autophagy proteins in terms of puncta formation and demonstrated that the ULK1 complex appears to be the most upstream unit, followed by the Atg14-containing PI3-kinase complex, DFCP1/WIPI-1, the Atg12 system and the LC3 system (**Fig. 8**). The basic hierarchy is similar to that of yeast Atg proteins,[10] but we defined the functional steps of higher eukaryote specific FIP200 and DFCP1. We further revealed that these autophagy factors gather at sites tightly associated with the ER, where VMP1 transiently localizes (**Fig. 8**). ULK1 and Atg14 localize to these sites in a manner responsive to starvation, even in the presence of wortmannin. We therefore postulate that these sites represent the mammalian autophagosome formation sites, which may be equivalent to the yeast PAS.

One notable finding in this hierarchical analysis is that Atg14 punctate structures are not generated in FIP200 KO cells (**Fig. 5A**). Since it has already been shown that Beclin 1 can be regulated by Bcl-2 through direct binding in a nutrient-dependent manner,[42-44] the Beclin 1-Atg14-containing PI3-kinase complex appears to be regulated by two major nutrient signaling pathways from mTOR-ULK1 and Bcl-2. Another interesting observation is that, although localizations of the two PI(3)P-interacting proteins, DFCP1 and WIPI-1 is different, they are both controlled by the ULK1 and Atg14 complexes. However, it is not clear how Atg14 influences the translocation of DFCP1, which seems to take place on a separate structure, perhaps on the ER membrane.[31] We and others have previously observed that, in addition to the punctate structures, some Atg14 appears in a reticular pattern[25] and these structures likely represent the ER.[26] It is possible that these two different populations of the Atg14 complex (diffuse ER and punctate pattern) produce PI(3)P on distinct membranes, to which DFCP1 and WIPI-1 target.

Despite recent progress in elucidating the molecular mechanisms of autophagosome formation, the origin of the isolation membrane remains unanswered. Nonetheless, there have been several lines of evidence suggesting involvement of the ER in autophagosome formation. The isolation membrane has been proposed to be differentiated from the ER,[11] and indeed, the developing isolation membrane is often associated with and directly connected to the rough ER.[32,33,45,46] Studies in yeast have shown that early secretory pathway proteins are required for yeast autophagosome formation.[47-49] In addition, the ER-targeted, but not mitochondrial-targeted, Bcl-2 suppresses autophagy by sequestering Beclin 1.[42,50] Finally, DFCP1 translocates from the ER to LC3-associated omegasome.[31]

In the present study, we showed that the early autophagic structures associate with the ER, supporting the idea that the ER plays a critical role in autophagosome formation. However, it remains unknown whether these ULK1-Atg14 structures represent some special site of the ER membrane itself or some unknown distinct structure that tightly associates with the ER. This site appears to be composed of at least two different components, because localization of DFCP1 and other Atg proteins are distinct, although they are frequently in close proximity to each other (**Fig. 1K**).

Our further analysis revealed that VMP1 transiently associates with the very early autophagic structures (**Fig. 7**). However, the functional step of VMP1 appears not to be upstream of Atg proteins, because VMP1 silencing causes accumulation of abnormal autophagic membranes containing ULK1, WIPI-1, DFCP1 and Atg16L1 (**Fig. 7H**). Although it was reported that VMP1 interacts with Beclin 1, the phenotype of VMP1 siRNA was different from that of PI3-kinase suppression by wortmannin. In addition, most of Beclin 1 was not co-fractionated with VMP1 (**Fig. 7B**). These results suggest that primary function of VMP1 in the autophagy pathway is not through regulation of PI3-kinase activity. VMP1 may provide essential component(s) that are required for a later stage of autophagosome formation. Further analysis will be required to elucidate the role of VMP1 in autophagosome formation.

Materials and Methods

Cell culture and transfection. MEFs (mouse embryonic fibroblasts), HeLa and HepG2 cells were cultured in Dulbecco's modified Eagle's medium (DMEM) supplemented with 10% FBS, 50 μg/ml penicillin and streptomycin in a 5% CO_2 incubator (regular medium). NIH3T3 cells were maintained in DMEM containing 10% bovine calf serum and the antibiotics (regular medium). Atg5 KO,[51] FIP200 KO,[52] and Atg3 KO[35] MEFs were generated previously. For starvation, cells were washed with PBS and incubated in amino acid-free DMEM without serum (starvation medium). FuGENE 6 reagent (Roche Applied Science, 1814443) was used for transfection. Wortmannin and puromycin were purchased from Sigma (P8833).

Plasmids. IMAGE Consortium cDNA clones encoding mouse DFCP1 (GenBank accession no. CB526501) and human VMP1 (GenBank accession no. BQ712360), an ORFeome collaboration clone (GenBank accession no. DQ891254) encoding human ERGIC53, and a TOYOBO cDNA clone (GenBank accession no. NM_006364) encoding human Sec23A were obtained from Invitrogen (Clone ID: 6848683, 6301764), Promega (ORS09408) or TOYOBO (FCC172E08), respectively. Full length cDNA encoding human WIPI-1 was amplified by PCR from total cDNA of HeLa cells. To generate the pMXs-puro-GFP-DFCP1, pMXs-puro-GFP-WIPI-1, pMXs-puro-HA-WIPI-1, pMXs-puro-VMP1-GFP, pMXs-IP-GFP-Sec23A and pMXs-IP-spGFP-ERGIC53 plasmids, cDNAs were cloned into pMXs-puro or pMXs-IP (provided by T. Kitamura, University of Tokyo, Tokyo, Japan) (Kitamura et al. 2003) together with EGFP (Clontech, Mountain View, CA), mRFP (provided by R.Y. Tsien, University of California, San Diego),[53] and 3xHA fragments. pMXs-IP-GFP-LC3, pMXs-IP-GFP-ULK1, pMXs-IP-HA-ULK1, pMXs-IP-GFP-Atg14, pMXs-puro-HA-Atg14, pMXs-IP-GFP-Atg5 and pMXs-puro-Vps34-GFP have been previously described.[18,25] To construct mRFP-ER and GEP-ER, a cDNA of rat cytochrome b5 encoding residues 95–134 (provided by K. Mihara, Kyushu University, Fukuoka, Japan) was subcloned into pMXs-puro-mRFP and pMXs-puro-GFP.

Retroviral infections and generation of stable cell lines. Stable cell lines were generated using a retroviral expression system as previously described.[18] Briefly, Plat E cells (provided by T. Kitamura) were transiently transfected with pMXs vectors using FuGENE 6 reagent. After 72 hours of culture, the growth medium containing retrovirus was collected. MEFs and NIH3T3 cells were incubated with the collected virus-containing medium with 8 μg/ml polybrene for 24 hours. Uninfected cells were removed by puromycin selection.

Antibodies. Mouse monoclonal anti-HA (16B12) antibodies were purchased from Covance Research Products (MMS-101R). Rat monoclonal anti-GFP antibodies (GF090R) were purchased from Nacalai Tesque (04404-84). The rabbit polyclonal antibodies against Beclin 1,[25] LC3 (SK2-6)[54] and Atg16L1[55] were described previously. Mouse monoclonal anti-GM130 and anti-HSP90 antibodies were purchased from BD bioscience (G65120, 610419). Rabbit polyclonal anti-Lamp1 antibodies were provided by Y. Tanaka (Kyushu University, Fukuoka, Japan).[56] Rabbit polyclonal andibodies against TOM70 were provided by K. Mihara (Kyushu University, Fukuoka, Japan).[57] Mouse monoclonal anti-Syntaxin 6 antibodies were purchased from Abcam (ab12370). Rabbit polyclonal anti-PDI antibodies were described previously.[58] Guinea pig polyclonal anti-p62 antibodies were purchased from Progen (GP62-C).

Immunocytochemistry. Cells grown on cover slips were washed with PBS and fixed in 4% paraformaldehyde in PBS for 10 minutes at 4°C. Fixed cells were permeabilized with 50 μg/ml digitonin in PBS for 5 minutes, blocked with 3% BSA in PBS for 30 minutes and incubated with primary antibodies for 1 hour. After washing, cells were incubated with AlexaFluor 488-conjugated goat anti-rat, anti-rabbit or anti-mouse IgG or AlexaFluor 564-conjugated goat anti-rabbit or anti-mouse IgG secondary antibodies (Invitrogen) for 30 minutes and examined under a fluorescence microscope (IX81; Olympus) equipped with a CCD camera (ORCA ER, Hamamatsu Photonics). Linescan analysis

was performed using MetaMorph image analysis software version 7.0 (Molecular Devices). The pixel intensity in each channel was plotted against the position along a straight line across the dual image. 3D reconstruction from a series of confocal images (FV1000, Olympus) taken at 0.1 μm intervals and analyzed by FV10-ASW software (Olympus).

Fluorescence microscopy and time-lapse imaging. Fluorescence microscopy was performed with a microscope (IX81) equipped with a CCD camera (ORCA ER, Hamamatsu Photonics). An Olympus 60x PlanAPO oil immersion lens (numerical aperture, 1.42) was used. For time-lapse analysis, cells were plated onto a glass bottom dish and mounted in a chamber for live recording, and conditions maintained with 5% CO_2 at 37°C. Data were analyzed using MetaMorph image analysis software version 7.0 (Molecular Devices).

RNA Interference. Stealth RNAi oligonucleotides (Invitrogen) against human Atg14 and Vps34 were used for siRNA experiments as previously described.[25] The sequences used for VMP1 siRNA were as follows: human VMP1 siRNA antisense, 5'-UAU ACG UUG CAC AUA CUG UUG AUG C-3', sense, 5'-GCA UCA ACA GUA UGU GCA ACG UAU A-3'. For a negative control, a Medium GC duplex of stealth RNAi Negative Control Duplexes (Invitrogen, 12935-300) was used. The Stealth RNAi oligonucleotides were transfected into cells using Lipofectamine RNAiMAX (Invitrogen, 13778-150) according to the manufacturer's protocols. After 2 days, the cells were again transfected with the same siRNA and cultured for an additional 3 days before analysis, unless otherwise specified.

Subcellular fractionation. MEFs were cultured and harvested using 0.5% trypsin-EDTA. Cells were resuspended in regular medium and pelleted. Cell pellets were resuspended in homogenization buffer (20 mM HEPES (pH 7.4), 0.22 M mannitol, 0.07 M sucrose, 0.5 mM EDTA, 0.5 mM PMSF, 10 μg/ml soybean trypsin inhibitor, and Complete protease inhibitors mixture (Roche Applied Science, 11873580001)) and passaged 20 times through a 27-gauge needle. Post-nuclear supernatant (PNS) was prepared by two consecutive centrifugations at 500 x *g*. The PNS was placed onto 11 ml of a linear 5–30% OptiPrep gradient (Sigma, D1556) prepared in homogenization buffer at 4°C. Gradients were centrifuged at 38,000 rpm for 12 hours at 4°C using a Beckman SW41 rotor. Fourteen fractions (0.75 ml each) were carefully collected from the top of the gradient. Immunoblot analyses were performed using antibodies against individual organelle markers as indicated.

Quantitative PCR. Real-Time PCR was performed as previously described.[25] The primer sets used were as follows: human VMP1 forward, 5'-TGG GCA CAC CAC AGG GAG AA-3' and reverse, 5'-CCG CTG CTG GAT TCG TTT GG-3' and human β-actin forward, 5'-ATT GCC GAC AGG ATG CAG AA-3' and reverse, 5'-ACA TCT GCT GGA AGG TGG ACA G-3'.

Acknowledgements

We thank Dr. Masaaki Komatsu (Tokyo Metropolitan Institute of Medical Science) for providing Atg3 KO MEFs, Dr. Roger Y. Tsien (University of California at San Diego) for mRFP cDNA, Dr. Katsuyoshi Mihara (Kyushu University) for rat cytochrome b5 cDNA, Dr. Toshio Kitamura (The University of Tokyo) for the retroviral vectors and Plat-E cells, Dr. Yoshitaka Tanaka (Kyushu University) for anti-Lamp1 antibodies, and Dr. Jun-Lin Guan (University of Michigan) for FIP200 KO cells. We also thank Dr. Naotada Ishihara for helpful discussions. This work was supported in part by Grants-in-Aid for Scientific Research from the Ministry of Education, Culture, Sports, Science and Technology, Japan (to N.M.), and grants for research fellowships from the Japan Society for the Promotion of Science for Young Scientists (to E.I.), the Toray Science Foundation and the Takeda Science Foundation (to N.M.).

Note

Supplementry materials can be found at:
www.landesbioscience.com/supplement/ItakuraAUTO6-6-Sup.pdf
www.landesbioscience.com/supplement/ItakuraAUTO6-6-Mov1.mov
www.landesbioscience.com/supplement/ItakuraAUTO6-6-Mov2.mov

References

1. Rubinsztein DC. The roles of intracellular protein-degradation pathways in neurodegeneration. Nature 2006; 443:780-6.
2. Mizushima N. Autophagy: process and function. Genes Dev 2007; 21:2861-73.
3. Mizushima N, Levine B, Cuervo AM, Klionsky DJ. Autophagy fights disease through cellular self-digestion. Nature 2008; 451:1069-75.
4. Cecconi F, Levine B. The role of autophagy in mammalian development: cell makeover rather than cell death. Dev Cell 2008; 15:344-57.
5. Virgin HW, Levine B. Autophagy genes in immunity. Nat Immunol 2009; 10:461-70.
6. Deretic V. Multiple regulatory and effector roles of autophagy in immunity. Curr Opin Immunol 2009; 21:53-62.
7. Xie Z, Klionsky DJ. Autophagosome formation: core machinery and adaptations. Nat Cell Biol 2007; 9:1102-9.
8. Suzuki K, Ohsumi Y. Molecular machinery of autophagosome formation in yeast, *Saccharomyces cerevisiae*. FEBS Lett 2007; 581:2156-61.
9. Longatti A, Tooze SA. Vesicular trafficking and autophagosome formation. Cell Death Differ 2009; 16:956-65.
10. Suzuki K, Kubota Y, Sekito T, Ohsumi Y. Hierarchy of Atg proteins in pre-autophagosomal structure organization. Genes Cells 2007; 12:209-18.
11. Dunn WA Jr. Studies on the mechanisms of autophagy: formation of the autophagic vacuole. J Cell Biol 1990; 110:1923-33.
12. Yamamoto A, Masaki R, Tashiro Y. Characterization of the isolation membranes and the limiting membranes of autophagosomes in rat hepatocytes by lectin cytochemistry. J Histochem Cytochem 1990; 38:573-80.
13. Noda T, Suzuki K, Ohsumi Y. Yeast autophagosomes: de novo formation of a membrane structure. Trends Cell Biol 2002; 12:231-5.
14. Suzuki K, Kirisako T, Kamada Y, Mizushima N, Noda T, Ohsumi Y. The pre-autophagosomal structure organized by concerted functions of *APG* genes is essential for autophagosome formation. EMBO J 2001; 20:5971-81.
15. Kim J, Huang WP, Stromhaug PE, Klionsky DJ. Convergence of multiple autophagy and cytoplasm to vacuole targeting components to a perivacuolar membrane compartment prior to de novo vesicle formation. J Biol Chem 2002; 277:763-73.
16. Meijer WH, van der Klei IJ, Veenhuis M, Kiel JAKW. *ATG* genes involved in non-selective autophagy are conserved from yeast to man, but the selective Cvt and pexophagy pathways also require organism-specific genes. Autophagy 2007; 3:106-16.
17. Chan EYW, Tooze SA. Evolution of Atg1 function and regulation. Autophagy 2009; 5:758-65.
18. Hara T, Takamura A, Kishi C, Iemura S, Natsume T, Guan JL, Mizushima N. FIP200, a ULK-interacting protein, is required for autophagosome formation in mammalian cells. J Cell Biol 2008; 181:497-510.
19. Chan EYW, Longatti A, McKnight NC, Tooze SA. Kinase-inactivated ULK proteins inhibit autophagy via their conserved C-terminal domain using an Atg13-independent mechanism. Mol Cell Biol 2009; 29:157-71.
20. Hosokawa N, Hara T, Kaizuka T, Kishi C, Takamura A, Miura Y, et al. Nutrient-dependent mTORC1 association with the ULK1-Atg13-FIP200 complex required for autophagy. Mol Biol Cell 2009; 20:1981-91.

21. Jung CH, Jun CB, Ro SH, Kim YM, Otto NM, Cao J, et al. ULK-Atg13-FIP200 complexes mediate mTOR signaling to the autophagy machinery. Mol Biol Cell 2009; 20:1992-2003.
22. Ganley IG, Lam DH, Wang J, Ding X, Chen S, Jiang X. ULK1-ATG13-FIP200 complex mediates mTOR signaling and is essential for autophagy. J Biol Chem 2009; 284:12297-305.
23. Mercer CA, Kaliappan A, Dennis PB. A novel, human Atg13 binding protein, Atg101, interacts with ULK1 and is essential for macroautophagy. Autophagy 2009; 5:649-62.
24. Hosokawa N, Sasaki T, Iemura S, Natsume T, Hara T, Mizushima N. Atg101, a novel mammalian autophagy protein interacting with Atg13. Autophagy 2009; 5:973-9.
25. Itakura E, Kishi C, Inoue K, Mizushima N. Beclin 1 forms two distinct phosphatidylinositol 3-kinase complexes with mammalian Atg14 and UVRAG. Mol Biol Cell 2008; 19:5360-72.
26. Matsunaga K, Saitoh T, Tabata K, Omori H, Satoh T, Kurotori N, et al. Two Beclin 1-binding proteins, Atg14L and Rubicon, reciprocally regulate autophagy at different stages. Nat Cell Biol 2009; 11:385-96.
27. Zhong Y, Wang QJ, Li X, Yan Y, Backer JM, Chait BT, et al. Distinct regulation of autophagic activity by Atg14L and Rubicon associated with Beclin 1-phosphatidylinositol-3-kinase complex. Nat Cell Biol 2009; 11:468-76.
28. Sun Q, Fan W, Chen K, Ding X, Chen S, Zhong Q. Identification of Barkor as a mammalian autophagy-specific factor for Beclin 1 and class III phosphatidylinositol 3-kinase. Proc Natl Acad Sci USA 2008; 105:19211-6.
29. Proikas-Cezanne T, Waddell S, Gaugel A, Frickey T, Lupas A, Nordheim A. WIPI-1a (WIPI49), a member of the novel 7-bladed WIPI protein family, is aberrantly expressed in human cancer and is linked to starvation-induced autophagy. Oncogene 2004; 23:9314-25.
30. Mizushima N, Yoshimori T, Ohsumi Y. Role of the Apg12 conjugation system in mammalian autophagy. Int J Biochem Cell Biol 2003; 35:553-61.
31. Axe EL, Walker SA, Manifava M, Chandra P, Roderick HL, Habermann A, et al. Autophagosome formation from membrane compartments enriched in phosphatidylinositol 3-phosphate and dynamically connected to the endoplasmic reticulum. J Cell Biol 2008; 182:685-701.
32. Yla-Anttila P, Vihinen H, Jokitalo E, Eskelinen EL. 3D tomography reveals connections between the phagophore and endoplasmic reticulum. Autophagy 2009; 5.
33. Hayashi-Nishino M, Fujita N, Noda T, Yamaguchi A, Yoshimori T, Yamamoto A. A subdomain of the endoplasmic reticulum forms a cradle for autophagosome formation. Nat Cell Biol 2009.
34. Mizushima N, Yamamoto A, Hatano M, Kobayashi Y, Kabeya Y, Suzuki K, et al. Dissection of autophagosome formation using Apg5-deficient mouse embryonic stem cells. J Cell Biol 2001; 152:657-67.
35. Sou YS, Waguri S, Iwata J, Ueno T, Fujimura T, Hara T, et al. The Atg8 conjugation system is indispensable for proper development of autophagic isolation membranes in mice. Mol Biol Cell 2008; 19:4762-75.
36. Kovács, AL, Réz, G, Pálfia, Z, Kovács, J. Autophagy in the epithelial cells of murine seminal vesicle in vitro. Formation of large sheets of nascent isolation membranes, sequestration of the nucleus and inhibition by wortmannin and 3-methyladenine. Cell Tissue Res 2000; 302:253-61.
37. Ropolo A, Grasso D, Pardo R, Sacchetti ML, Archange C, Lo Re A, et al. The pancreatitis-induced vacuole membrane protein 1 triggers autophagy in mammalian cells. J Biol Chem 2007; 282:37124-33.
38. Dusetti NJ, Jiang Y, Vaccaro MI, Tomasini R, Azizi Samir A, Calvo EL, et al. Cloning and expression of the rat vacuole membrane protein 1 (VMP1), a new gene activated in pancreas with acute pancreatitis, which promotes vacuole formation. Biochem Biophys Res Commun 2002; 290:641-9.
39. Calvo-Garrido J, Carilla-Latorre S, Lázaro-Diéguez, F, Egea G, Escalante R. Vacuole membrane protein 1 is an endoplasmic reticulum protein required for organelle biogenesis, protein secretion and development. Mol Biol Cell 2008; 19:3442-53.
40. Calvo-Garrido J, Escalante R. Autophagy dysfunction and ubiquitin-positive protein aggregates in Dictyostelium cells lacking Vmp1. Autophagy 2010; 6.
41. Bjørkøy G, Lamark T, Brech A, Outzen H, Perander M, Øvervatn A, et al. p62/SQSTM1 forms protein aggregates degraded by autophagy and has a protective effect on huntingtin-induced cell death. J Cell Biol 2005; 171:603-14.
42. Pattingre S, Tassa A, Qu X, Garuti R, Liang XH, Mizushima N, et al. Bcl-2 antiapoptotic proteins inhibit Beclin 1-dependent autophagy. Cell 2005; 122:927-39.
43. Maiuri MC, Le Toumelin G, Criollo A, Rain JC, Gautier F, Juin P, et al. Functional and physical interaction between Bcl-X(L) and a BH3-like domain in Beclin-1. EMBO J 2007; 26:2527-39.
44. Wei Y, Pattingre S, Sinha S, Bassik M, Levine B. JNK1-mediated phosphorylation of Bcl-2 regulates starvation-induced autophagy. Mol Cell 2008; 30:678-88.
45. Eskelinen EL. Maturation of autophagic vacuoles in mammalian cells. Autophagy 2005; 1:1-10.
46. Kovács AL, Pálfia Z, Réz G, Vellai T, Kávacs J. Sequestration revisited: integrating traditional electron microscopy, de novo assembly and new results. Autophagy 2007; 3:655-62.
47. Ishihara N, Hamasaki M, Yokota S, Suzuki K, Kamada Y, Kihara A, et al. Autophagosome requires specific early Sec proteins for its formation and NSF/SNARE for vacuolar fusion. Mol Biol Cell 2001; 12:3690-702.
48. Hamasaki M, Noda T, Ohsumi Y. The early secretory pathway contributes to autophagy in yeast. Cell Struct Funct 2003; 28:49-54.
49. Reggiori F, Wang CW, Nair U, Shintani T, Abeliovich H, Klionsky DJ. Early stages of the secretory pathway, but not endosomes, are required for Cvt vesicle and autophagosome assembly in *Saccharomyces cerevisiae*. Mol Biol Cell 2004; 15:2189-204.
50. Criollo A, Maiuri MC, Tasdemir E, Vitale I, Fiebig AA, Andrews D, et al. Regulation of autophagy by the inositol trisphosphate receptor. Cell Death Differ 2007; 14:1029-39.
51. Kuma A, Hatano M, Matsui M, Yamamoto A, Nakaya H, Yoshimori T, et al. The role of autophagy during the early neonatal starvation period. Nature 2004; 432:1032-6.
52. Gan B, Peng X, Nagy T, Alcaraz A, Gu H, Guan JL. Role of FIP200 in cardiac and liver development and its regulation of TNFα and TSC-mTOR signaling pathways. J Cell Biol 2006; 175:121-33.
53. Campbell RE, Tour O, Palmer AE, Steinbach PA, Baird GS, Zacharias DA, Tsien RY. A monomeric red fluorescent protein. Proc Natl Acad Sci USA 2002; 99:7877-82.
54. Kabeya Y, Mizushima N, Ueno T, Yamamoto A, Kirisako T, Noda T, et al. LC3, a mammalian homologue of yeast Apg8p, is localized in autophagosome membranes after processing. EMBO J 2000; 19:5720-8.
55. Mizushima N, Kuma A, Kobayashi Y, Yamamoto A, Matsubae M, Takao T, et al. Mouse Apg16L, a novel WD-repeat protein, targets to the autophagic isolation membrane with the Apg12-Apg5 conjugate. J Cell Sci 2003; 116:1679-88.
56. Niwa K, Tanaka R, Murase H, Ishikawa T, Fujita H, Himeno M, Tanaka Y. Two lysosomal membrane proteins, LGP85 and LGP107, are delivered to late endosomes/lysosomes through different intracellular routes after exiting from the trans-Golgi network. Biochem Biophys Res Commun 2003; 301:833-40.
57. Suzuki H, Maeda M, Mihara K. Characterization of rat TOM70 as a receptor of the preprotein translocase of the mitochondrial outer membrane. J Cell Sci 2002; 115:1895-905.
58. Akagi S, Yamamoto A, Yoshimori T, Masaki R, Ogawa R, Tashiro Y. Distribution of protein disulfide isomerase in rat hepatocytes. J Histochem Cytochem 1988; 36:1533-42.